

Folding simulations of gramicidin A into the β -helix conformations: Simulated annealing molecular dynamics study

Takaharu Mori^{1,2,a)} and Yuko Okamoto^{1,2,a)}

¹Department of Physics, School of Science, Nagoya University, Furo-cho, Chikusa-ku, Nagoya, Aichi 464-8602, Japan

²Institute for Bioinformatics Research and Development (BIRD), Japan Science and Technology Agency (JST), Furo-cho, Chikusa-ku, Nagoya, Aichi 464-8602, Japan

(Received 17 April 2009; accepted 22 September 2009; published online 27 October 2009)

Gramicidin A is a linear hydrophobic 15-residue peptide which consists of alternating D- and L-amino acids and forms a unique tertiary structure, called the $\beta^{6.3}$ -helix, to act as a cation-selective ion channel in the natural conditions. In order to investigate the intrinsic ability of the gramicidin A monomer to form secondary structures, we performed the folding simulation of gramicidin A using a simulated annealing molecular dynamics (MD) method in vacuum mimicking the low-dielectric, homogeneous membrane environment. The initial conformation was a fully extended one. From the 200 different MD runs, we obtained a right-handed $\beta^{4.4}$ -helix as the lowest-potential-energy structure, and left-handed $\beta^{4.4}$ -helix, right-handed and left-handed $\beta^{6.3}$ -helix as local-minimum energy states. These results are in accord with those of the experiments of gramicidin A in homogeneous organic solvent. Our simulations showed a slight right-hand sense in the lower-energy conformations and a quite β -sheet-forming tendency throughout almost the entire sequence. In order to examine the stability of the obtained right-handed $\beta^{6.3}$ -helix and $\beta^{4.4}$ -helix structures in more realistic membrane environment, we have also performed all-atom MD simulations in explicit water, ion, and lipid molecules, starting from these β -helix structures. The results suggested that $\beta^{6.3}$ -helix is more stable than $\beta^{4.4}$ -helix in the inhomogeneous, explicit membrane environment, where the pore water and the hydrogen bonds between Trp side-chains and lipid-head groups have a role to further stabilize the $\beta^{6.3}$ -helix conformation. © 2009 American Institute of Physics.

[doi:10.1063/1.3247578]

I. INTRODUCTION

Gramicidin A is a linear hydrophobic 15-residue peptide which consists of alternating D- and L-amino acids, and the amino-acid sequence is as follows: HCO-Val-Gly-Ala-D-Leu-Ala-D-Val-Val-D-Val-Trp-D-Leu-Trp-D-Leu-Trp-D-Leu-Trp-NHCH₂CH₂OH. Because of the structural flexibility of gramicidin A, it forms various conformations depending on the solvent, concentration, and temperature.^{1,2} For example, in water, gramicidin A forms a disordered (random-coil) conformation because of its low solubility. In organic solvents, gramicidin A forms random-coil or helical conformations such as $\beta^{4.4}$ -helix and $\beta^{6.3}$ -helix in a monomeric state or double-stranded helical dimer ($\pi\pi$ -helix).³⁻⁷ In the lipid membrane, gramicidin A adopts a cation selective ion channel of the right-handed head-to-head single-stranded $\beta^{6.3}$ -helical dimer.⁸

Gramicidin A is one of the best characterized membrane peptides, both experimentally and theoretically.⁹ Computer simulations have played an important role in providing useful information about structures and functions of gramicidin A at the atomic level. However, many theoretical studies have mainly focused on the channel structure (dimeric state) and functions such as ion selectivity, permeability, and chan-

nel gating,¹⁰⁻¹² while the β -helix-formation mechanism, origin of its right-hand sense, or the inherent ability of the secondary-structure formation of the monomer has yet to be clarified. Moreover, no one has carried out a successful folding simulation of gramicidin A into the β -helix conformation, using only the amino-acid sequence information.

In this article, we present the results of folding simulations of the gramicidin A monomer using a simulated annealing molecular dynamics (MD) method.¹³ The initial conformation was a fully extended one. Because gramicidin A forms various conformations depending on the solvent, we carried out the folding simulations in vacuum to investigate what kind of conformations inherently exists in the lowest and local-minimum energy states. From the simulations, several β -helix conformations were successfully obtained in lower energy states as experimentally observed in organic solvents and membranes. We further examined the stability of the $\beta^{4.4}$ -helix and $\beta^{6.3}$ -helix conformations in explicit, more realistic membrane environment from all-atom MD simulations to discuss why gramicidin A forms the particular conformation, the $\beta^{6.3}$ -helix, in the membrane.

II. MATERIALS AND METHODS

A. Folding simulation of the gramicidin A monomer

Simulated annealing MD simulations of the gramicidin A monomer were carried out by using the CHARMM (Chem-

^{a)}Electronic addresses: tmori@tb.phys.nagoya-u.ac.jp and okamoto@phys.nagoya-u.ac.jp.

istry at HARvard Macromolecular Mechanics) program package version c32b2 and using the PARAM22 version of the CHARMM empirical energy function.^{14,15} Starting from a fully extended conformation (namely, the backbone dihedral angles are set $\phi, \psi=180^\circ$), energy minimization was carried out to remove the initial strains. We then performed MD simulations as follows: heating the system from 300 to 1200 K in 1.01 ps, followed by cooling linearly from 1200 to 250 K in 10 ns with an increment of 50 K (500 ps canonical MD simulations were performed at each of 20 temperature values). We utilized the Gaussian thermostat for the temperature control algorithm implemented in CHARMM and the leap-frog integration method with a time step of 1 fs.^{16–18} A 20 Å cutoff distance was used for the calculation of nonbonded interaction energies. The dielectric constant ϵ of the solute-surrounding environment was set to one (vacuum) to mimic the effect of the low-dielectric hydrophobic core of membranes ($\epsilon=2-4$), whereas that for bulk water is 78. We performed 200 simulation runs with different random number seeds.

B. All-atom MD simulations of the β -helix in the membrane

In order to investigate the structural stability of the β -helix conformations in the membrane, we also carried out all-atom model MD simulations of the right-handed $\beta^{4,4}$ -helix and $\beta^{6,3}$ -helix in explicit water, ion, and lipid molecules using the NAMD2 program.¹⁹ The lowest-potential-energy structure obtained from the above folding simulations and the NMR structure (PDB: 1MAG; Chain A) were used for the right-handed $\beta^{4,4}$ -helix and the right-handed $\beta^{6,3}$ -helix, respectively. The initial structure of the peptide-membrane complex was constructed as follows. First, we prepared the equilibrated 1,2-dimyristoyl-*sn*-glycero-3-phosphorylcholine (DMPC) bilayer structure (128 lipids with the area per lipid of 60.7 Å² and 3819 water molecules), which was downloaded from the CHARMM-GUI Website.^{20,21} We then inserted the peptide into the DMPC bilayer, after removing four lipid molecules from the top leaflet to minimize the volume change. The peptide was placed at the membrane interface and perpendicular to the membrane plane. Steric collisions between peptide and lipids were reduced by moving lipid molecules as rigid bodies. We then added a 150 mM NaCl solution to the system. The system contains 124 lipids, 7820 water molecules, 22 Na⁺, and 22 Cl⁻, and the box size of the initial structure was 64 × 64 × 95 Å³ for both the simulations of $\beta^{4,4}$ -helix and $\beta^{6,3}$ -helix.

The systems were subjected to 10 000-step energy minimization with the harmonic restraints of 10.0 kcal/mol Å² on the heavy atoms of peptide and lipids and 1.0 kcal/mol Å² on ions in the bulk water to remove steric clashes in the initial structure, followed by 1 ns MD simulations for the equilibration. For the first 200 ps, MD simulation in a canonical (NVT) ensemble was performed with the same constraints used in the minimization. We then carried out the 200 ps simulation in the isothermal-isobaric (NPT) ensemble with the harmonic positional restraints of

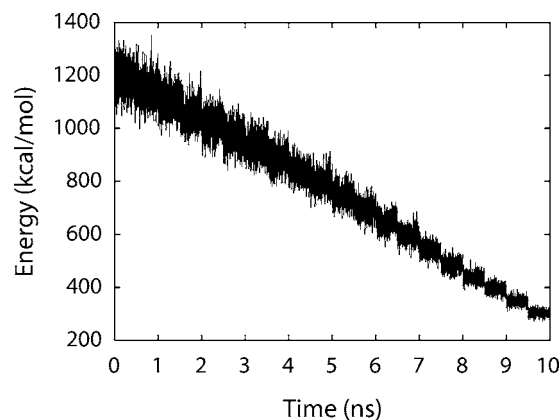


FIG. 1. Time course of the total potential energy of gramicidin A obtained in a simulated annealing MD simulation.

1.0 kcal/mol Å² on the heavy atoms of peptide and 10.0 kcal/mol Å² on the direction of lipid head groups normal to the bilayer to avoid drastic undulations of the lipid bilayer. For the final 400 ps, harmonic positional restraints of 1.0 kcal/mol Å² were applied on the heavy atoms of peptide, and these restraints were gradually reduced to zero. A 20 ns MD simulation was then carried out in the constant area isothermal-isobaric (NPAT) ensemble for the production runs without any restraints on the system. In these simulations, constant pressure (1 atm) and constant temperature (300 K) were maintained using Langevin dynamics and Langevin piston, respectively. The particle mesh Ewald method was employed for the calculation of the electrostatic interactions.²²

III. RESULTS AND DISCUSSION

A. Folding simulations of the gramicidin A monomer in vacuum

Figure 1 shows the time course of the total potential energy obtained in one of the simulated annealing MD runs. We observe good decrease in the potential energy during the simulation. We selected the lowest-energy structure from each MD run, namely, 200 structures in total, for subsequent analyses.

The 20 lowest-energy structures of the 200 obtained conformations are shown in Fig. 2. We found that the lowest-potential-energy conformation is a right-handed $\beta^{4,4}$ -helix (the total potential energy was 261.5 kcal/mol). Left-handed $\beta^{4,4}$ -helix, right-handed $\beta^{6,3}$ -helix, and left-handed $\beta^{6,3}$ -helix were also obtained, and the lowest potential energy of each conformation was 268.4, 269.9, and 283.4 kcal/mol, respectively. The root-mean-square deviation (RMSD) for C α atoms between the NMR structure (PDB code: 1MAG) and the obtained right-handed $\beta^{6,3}$ -helix (No. 12 in Fig. 2) is 1.3 Å, indicating the successful prediction of this conformation. In the total of 200 structures, we observed 18 right-handed $\beta^{4,4}$ -helix, 20 left-handed $\beta^{4,4}$ -helix, three right-handed $\beta^{6,3}$ -helix (two of which were partially frayed), and one left-handed $\beta^{6,3}$ -helix conformations. Thus, although the ratio of the right-handed and left-handed configurations obtained is about 1:1, the right-handed one is slightly predominant in the lower energy conformations (see Fig. 2). We also obtained

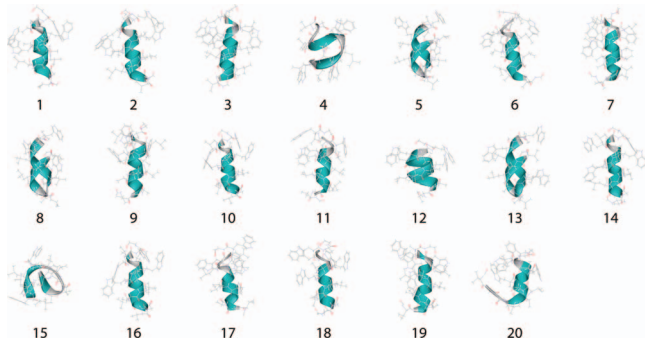


FIG. 2. The 20 lowest-energy conformations of gramicidin A obtained from 200 simulated annealing MD runs. Conformations are ordered in the increasing order of energy. Right-handed $\beta^{4,4}$ -helix: 1, 2, 3, 6, 7, 9, 10, 14, 16, and 18. Left-handed $\beta^{4,4}$ -helix: 11, 17, 19, and 20. Right-handed $\beta^{6,3}$ -helix: 12. β -hairpin: 4. Monomeric double-stranded β -helix: 5, 8, and 13.

other conformations such as β -hairpin (see No. 4 in Fig. 2) and monomeric double-stranded β -helix (see Nos. 5, 8, and 13 in Fig. 2). Although no experimental results have indicated the existence of these structures, the latter structure resembles the $\pi\pi$ -helix,⁷ which can be observed in the dimeric state. In our simulations, no α -helix conformation was observed, which is consistent with the fact that D-amino acids are α -helix breakers.²³ It is suggested that in the right-handed α -helix conformation steric clashes occur between C^β atom of D-amino acid in the i th residue and the carbonyl oxygen atoms of both the i th and $(i-1)$ th residues.²³

Table I lists the lowest total potential energy and its component energy values of the $\beta^{4,4}$ -helix, $\beta^{6,3}$ -helix, β -hairpin, and monomeric double-stranded β -helix structures obtained by the present simulations. Interestingly, the potential energy of each conformation is close to each other in spite of the large conformational differences between these structures, implying the considerable structural flexibility of gramicidin A. The $\beta^{4,4}$ -helix has slightly lower total potential energy than the $\beta^{6,3}$ -helix, and the energy differences between right-handed and left-handed configurations appear to be small. Similar tendencies are also observed in other studies using the molecular mechanics method for D, L-alternating peptides.²⁴

To investigate the secondary-structure-forming tendency of gramicidin A, we analyzed the backbone hydrogen bonds in the obtained 200 structures using DSSP program.²⁵ Figure 3 shows the forming tendency of β -sheet, turn, and bend

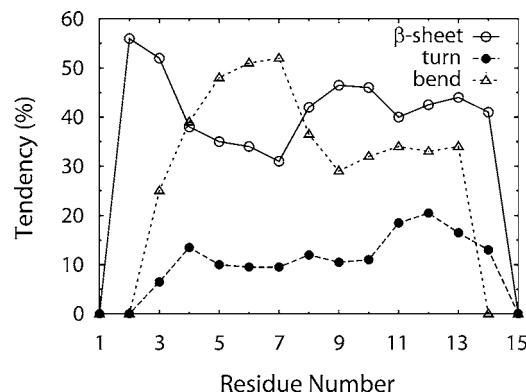


FIG. 3. Secondary-structure-forming tendencies of the gramicidin A monomer as a function of residue number. The results are mean values over the 200 obtained lowest-energy conformations. Open circles with solid line: β -sheet structure including both extended β -sheet and β -bridge, filled circles with dashed line: turn structure, and open triangles with dotted line: bend structure.

structures as a function of residue number. Because the DSSP program cannot directly distinguish β -helix from the extended β -sheet, the “ β -sheet structure” in Fig. 3 includes β -helix, extended β -sheet, and β -bridge structures. It is found that the β -sheet-forming tendency is 30%–50%, which is dominant over other conformations throughout almost the entire sequence. No α -helical or 3_{10} -helical hydrogen bonds were observed in any parts of the peptide, indicating the significant non- α -helicity in gramicidin A. The turn-forming tendency is 10%–20%, and the bend is highest near the middle of the sequence. This comes from the fact that in some MD runs gramicidin A formed the β -hairpinlike structures (but as higher-energy states), which had the bend structure rather than turn in the middle of the peptide.

To further investigate the secondary-structure propensity of gramicidin A, we computed the distributions of the backbone dihedral angles ϕ and ψ of all 200 structures. The definitions for the secondary-structure assignments of the Ramachandran plot of D-amino acids correspond to those of L-amino acids with the transformation from (ϕ, ψ) of L-amino acids to $(-\phi, -\psi)$. Figure 4 shows the results of the analysis, where the terminal residues Val 1 and Trp 15 were excluded from considerations and Gly 2 was treated as the D-amino acid because other even-numbered residues of gramicidin A are all D-amino acids. In this Figure, we see

TABLE I. The lowest total potential energy and its component energy term (in kcal/mol) of the $\beta^{4,4}$ -helix, $\beta^{6,3}$ -helix, β -hairpin, and monomeric double-stranded β -helix structures (LH: Left-handed conformation, RH: Right-handed conformation).

	RH- $\beta^{4,4}$ -helix	LH- $\beta^{4,4}$ -helix	RH- $\beta^{6,3}$ -helix	LH- $\beta^{6,3}$ -helix	β -hairpin	mds β -helix ^a
Total	261.5	268.4	269.9	283.4	265.6	267.3
Bond	61.9	64.4	60.0	73.2	64.3	71.9
Angle	99.4	81.7	88.1	93.4	95.7	83.8
Urey–Bradley	12.5	11.0	10.5	10.2	11.0	10.0
Dihedral	83.2	94.8	86.5	93.4	83.3	82.9
Improper	6.4	8.9	5.1	3.8	5.6	4.3
van der Waals	-47.0	-37.9	-26.0	-36.4	-43.6	-35.7
Coulomb	45.1	45.4	45.7	45.9	49.4	50.1

^aMonomeric double-stranded β -helix structure (see conformations 5, 8, and 13 in Fig. 2).

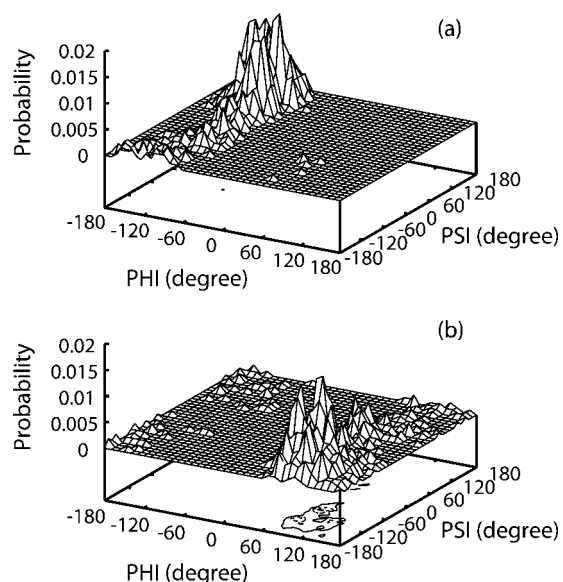


FIG. 4. Distributions of the backbone dihedral angles ϕ and ψ of gramicidin A. (a) L-amino acids and (b) D-amino acids.

greater distribution in the β -sheet region, indicating the strong tendency to form a β -sheet structure. The dihedral angles (ϕ, ψ) with the highest probability is $(80^\circ, -110^\circ)$ and $(-80^\circ, 110^\circ)$ for D-amino acids and L-amino acids, respectively. The distribution of the α -helical conformation is quite low, which is also consistent with the results of the hydrogen-bond analysis, as described above. Table II lists the average dihedral angles of the right-handed and left-handed conformations of $\beta^{4.4}$ -helix and $\beta^{6.3}$ -helix. Although these structures are greatly different in appearance, the values of the backbone dihedral angles are close to each other and have the same sign even between right-handed and left-handed conformations. These results suggest that gramicidin A can easily form both right-handed and left-handed conformations of the $\beta^{4.4}$ -helix or $\beta^{6.3}$ -helix when the backbone dihedral angles lie within the β -sheet region.

In the present study, we performed the folding simulations of gramicidin A in vacuum ($\epsilon=1$) to investigate what kind of conformations inherently exists in local-minimum energy states. The solvent dependence on the conformation of gramicidin A has been reported experimentally. It is suggested that gramicidin A exists in equilibrium states between $\beta^{6.3}$ -helix and disordered conformations in dimethylsulfoxide ($\epsilon \approx 46$),⁴ and forms the $\beta^{4.4}$ -helix conformations in trifluoro-

TABLE II. Averaged backbone dihedral angles ϕ and ψ of the right-handed and left-handed conformations of $\beta^{4.4}$ -helix and $\beta^{6.3}$ -helix (LH: Left-handed conformation, RH: Right-handed conformation).

	D-amino acids		L-amino acids	
	ϕ (deg)	ψ (deg)	ϕ (deg)	ψ (deg)
RH- $\beta^{4.4}$	120.2	-87.5	-92.9	116.3
LH- $\beta^{4.4}$	77.4	-103.3	-115.1	86.2
RH- $\beta^{6.3}$	112.0	-109.3	-114.8	88.8
LH- $\beta^{6.3}$	71.9	-118.0	-121.4	112.0

roethanol ($\epsilon \approx 27$).⁶ Although the dielectric constant of the solute-surrounding medium in our simulation is lower than those of these organic solvents, our results are in accord with these experiments. In the membrane environment, gramicidin A adopts a right-handed $\beta^{6.3}$ -helix and forms the cation selective ion channel. In our simulation, we partially reproduced the structural properties of gramicidin A in the membrane, namely, the right-hand sense, while the $\beta^{6.3}$ -helix was obtained as a local-minimum-energy structure, not the global minimum. In order to form a $\beta^{6.3}$ -helix structure it is necessary to construct a large hole (about 4 Å in diameter) inside the helix and this seems to be energetically disadvantageous for the nonbonded interactions. In fact, van der Waals energy of the $\beta^{6.3}$ -helix is higher than that of the $\beta^{4.4}$ -helix (see Table I). Stabilization of the $\beta^{6.3}$ -helix conformation in forming the ion channel would be achieved by filling the hole with ion and water molecules. Moreover, it is suggested that in the real membrane system, hydrogen bonds between Trp side chains and lipid polar heads and/or interfacial water molecules have an important role in stabilizing a single-stranded $\beta^{6.3}$ -helix conformation.²⁶

B. All-atom MD simulations of the β -helix in the membrane

In order to elucidate these specific interactions of gramicidin A in the membrane, we performed the all-atom MD simulations of the $\beta^{4.4}$ -helix and $\beta^{6.3}$ -helix for 20 ns with explicit water, ion, and lipid molecules. For the initial structure of the $\beta^{4.4}$ -helix, we used the lowest-potential-energy conformation obtained by our simulations (No. 1 in Fig. 2), and for the $\beta^{6.3}$ -helix we used the NMR structure (PDB: 1MAG; chain A), where the pore inside the $\beta^{6.3}$ -helix was filled with water molecules. Figures 5(a) and 5(b) show the snapshot of the final structure of $\beta^{4.4}$ -helix and $\beta^{6.3}$ -helix, respectively. During the simulation, both the $\beta^{4.4}$ -helix and $\beta^{6.3}$ -helix showed a low RMSD (~ 1.2 Å) [see Fig. 5(c)]. However, the analysis of the RMS fluctuations of the C^α atoms demonstrated that the flexibility of the $\beta^{4.4}$ -helix is slightly greater than that of the $\beta^{6.3}$ -helix, especially in the C-terminal half of the peptide [see Fig. 5(d)]. In the simulation, we observed hydrogen bonds between the side chain atoms of Trp 9, 11, 13, and 15 and lipid head group. Importantly, these hydrogen bonds were much more formed in the $\beta^{6.3}$ -helix than the $\beta^{4.4}$ -helix [compare Figs. 5(e) and 5(f)], suggesting that the $\beta^{6.3}$ -helix is likely stabilized by the hydrogen bonds with lipids than the $\beta^{4.4}$ -helix. These hydrogen-bonded interactions between gramicidin A and lipids may shift the conformational equilibrium toward the $\beta^{6.3}$ -helix in the membrane. Furthermore, we also performed a MD simulation of the $\beta^{6.3}$ -helix, where the pore was not filled with water in the initial structure, and we found that water molecules rushed into the pore during the equilibration. These results imply that once gramicidin A adopts the $\beta^{6.3}$ -helix at the membrane interface, water molecules of the pore also stabilize the $\beta^{6.3}$ -helix conformation.

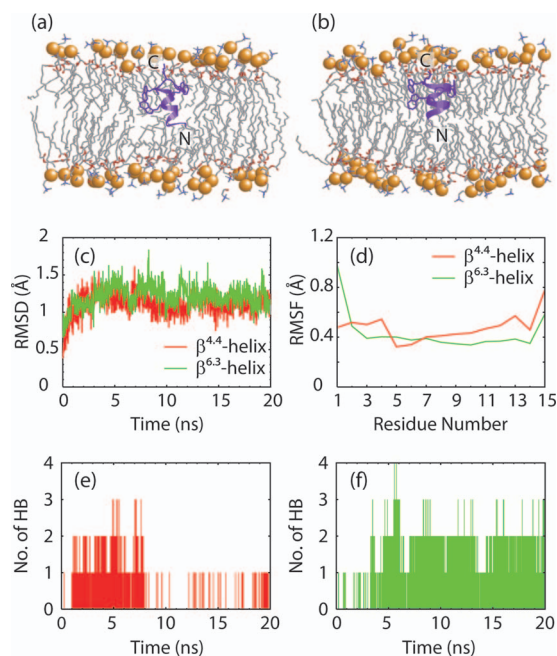


FIG. 5. Dynamical properties of $\beta^{4.4}$ -helix and $\beta^{6.3}$ -helix of the gramicidin A monomer in the explicit membrane environment. [(a) and (b)] Snapshot of the 20 ns structure of $\beta^{4.4}$ -helix (a) and $\beta^{6.3}$ -helix (b). Trp residues are represented by stick models. (c) Time courses of the RMSD of the C α atoms of $\beta^{4.4}$ -helix (in red) and $\beta^{6.3}$ -helix (in green) with respect to the initial structure. (d) Root-mean-square fluctuations (RMSF) of the C α atoms of $\beta^{4.4}$ -helix (in red) and $\beta^{6.3}$ -helix (in green). [(e) and (f)] Number of hydrogen bonds between side chain atoms of Trp 9, 11, 13, and 15 and lipid-head groups in $\beta^{4.4}$ -helix (e) and $\beta^{6.3}$ -helix (f).

IV. CONCLUSIONS

In this article, we showed that the folding simulations of gramicidin A successfully resulted in the characteristic tertiary structures, namely, the β -helices, using only the amino-acid sequence information. Our simulations demonstrated that gramicidin A forms various β -helical conformations, i.e., right-handed and left-handed $\beta^{4.4}$ -helix and $\beta^{6.3}$ -helix, in stable local-minimum energy states as experimentally observed in organic solvents and membranes. From the simulations, we suggest that the origin of the structural flexibility of gramicidin A comes from the fact that (i) several different conformations exist in lower-potential energy states, (ii) gramicidin A has a strong tendency to form a β -sheet structure but no α -helicity in any part of the peptide, and (iii) the energy differences and the backbone dihedral angle differences are small between the β -helical conformations. Therefore, the formation of the right-handed and left-handed configurations of the $\beta^{4.4}$ -helix and $\beta^{6.3}$ -helix would be easily achieved when the backbone dihedral angles lie within only the β -sheet region. We also performed the all-atom MD simulation of gramicidin A to discuss why the $\beta^{6.3}$ -helix is stable in the membrane. We found that the $\beta^{6.3}$ -helix is more stabilized than the $\beta^{4.4}$ -helix, where the pore water and the hydrogen bonds between Trp and lipid-head groups have a role to stabilize the $\beta^{6.3}$ -helix structure. These specific interactions between gramicidin A, lipids, and water molecules may shift the conformational equilibrium of gramicidin A toward the $\beta^{6.3}$ -helix to form the ion channel in the membrane.

In this study, we carried out the folding simulation of the gramicidin A monomer using the simulated annealing MD method. Because gramicidin A forms various conformations depending on the solvents, we carried out the simulations in vacuum to investigate the intrinsic ability of the peptide to form a secondary structure. We successfully obtained the stable β -helical conformations as observed in homogeneous organic solvents and membranes. This also indicates that the simulated annealing method is still useful to find out stable local-minimum energy structures for a small peptide such as gramicidin A. In this study, all-atom MD simulations were performed only to examine which conformations obtained in vacuum is actually stable in the membrane. Future work will be focused on the detailed mechanisms of the channel formation of gramicidin A using the all-atom MD simulation with explicit water and lipids.

ACKNOWLEDGMENTS

We would like to thank Yuji Sugita of RIKEN Advanced Science Institute for helpful discussions. The computation in this work was done using the supercomputer HPC2500 at Information Technology Center of Nagoya University. This research was supported in part by BIRD, Japan Science and Technology Agency (JST), and by the Grants-in-Aid for Scientific Research on Innovative Areas (“Fluctuations and Biological Functions”) and for the Next Generation Super Computing Project, Nanoscience Program from the Ministry of Education, Culture, Sports, Science and Technology, Japan.

- ¹R. E. Koeppe II and O. S. Anderson, *Annu. Rev. Biophys. Biomol. Struct.* **25**, 231 (1996).
- ²B. A. Wallace, *J. Struct. Biol.* **121**, 123 (1998).
- ³W. R. Veatch and E. R. Blout, *Biochemistry* **13**, 5257 (1974).
- ⁴G. E. Hawkes, L. Y. Lian, E. W. Randall, K. D. Sales, and E. H. Curzon, *Eur. J. Biochem.* **166**, 437 (1987).
- ⁵B. Roux, R. Bruschweiler, and R. R. Ernst, *Eur. J. Biochem.* **194**, 57 (1990).
- ⁶N. Abdul-Manan and J. F. Hinton, *Biochemistry* **33**, 6773 (1994).
- ⁷W. R. Veatch, E. T. Fossel, and E. R. Blout, *Biochemistry* **13**, 5249 (1974).
- ⁸A. S. Arseniev, I. L. Barsukov, V. F. Bystrov, A. L. Lomize, and Yu. A. Ovchinnikov, *FEBS Lett.* **186**, 168 (1985).
- ⁹O. S. Andersen, R. E. Koeppe II, and B. Roux, *IEEE Trans. Nanobiosci.* **4**, 10 (2005).
- ¹⁰B. Roux and M. Karplus, *Annu. Rev. Biophys. Biomol. Struct.* **23**, 731 (1994).
- ¹¹B. Roux, *Acc. Chem. Res.* **35**, 366 (2002).
- ¹²G. V. Miloshevsky and P. C. Jordan, *Biophys. J.* **86**, 92 (2004).
- ¹³S. Kirkpatrick, C. D. Gelatt, Jr., and M. P. Vecchi, *Science* **220**, 671 (1983).
- ¹⁴B. R. Brooks, R. E. Bruccoleri, B. D. Olafson, D. J. States, S. Swaminathan, and M. Karplus, *J. Comput. Chem.* **4**, 187 (1983).
- ¹⁵A. D. MacKerell Jr., D. Bashford, M. Bellott, R. L. Dunbrack Jr., J. D. Evanseck, M. J. Field, S. Fischer, J. Gao, H. Guo, S. Ha, D. Joseph-McCarthy, L. Kuchnir, K. Kuczera, F. T. K. Lau, C. Mattos, S. Michnick, T. Ngo, D. T. Nguyen, B. Prodhom, W. E. Reiher III, B. Roux, M. Schlenkrich, J. C. Smith, R. Stote, J. Straub, M. Watanabe, J. Wiorcikiewicz-Kuczera, D. Yin, and M. Karplus, *J. Phys. Chem. B* **102**, 3586 (1998).
- ¹⁶W. G. Hoover, A. J. C. Ladd, and B. Moran, *Phys. Rev. Lett.* **48**, 1818 (1982).
- ¹⁷D. J. Evans and G. P. Morriss, *Phys. Lett.* **98A**, 433 (1983).
- ¹⁸D. Brown and J. H. R. Clarke, *Mol. Phys.* **51**, 1243 (1984).
- ¹⁹L. Kalé, R. Skeel, M. Bhandarkar, R. Brunner, A. Gursoy, N. Krawetz, J. Phillips, A. Shinozaki, K. Varadarajan, and K. Schulten, *J. Comput. Phys.*

151, 283 (1999).

²⁰S. Jo, T. Kim, and W. Im, *PLoS ONE* **2**, e880 (2007).

²¹<http://www.charmm-gui.org>

²²T. Darden, D. York, and L. Pedersen, *J. Chem. Phys.* **98**, 10089 (1993).

²³R. Fairman, S. J. Anthonycahill, and W. F. Degrado, *J. Am. Chem. Soc.*

114, 5458 (1992).

²⁴H. Monoi, *Biophys. J.* **64**, 36 (1993).

²⁵W. Kabsch and C. Sander, *Biopolymers* **22**, 2577 (1983).

²⁶D. Salom, E. Perez-Paya, J. Pascal, and C. Abad, *Biochemistry* **37**, 14279 (1998).